

## ESR Spectra of Metal Oxide Catalysts During Propylene Oxidation\*

K. M. SANCIER, T. DOZONO†, AND H. WISE

*Solid State Catalysis Laboratory, Stanford Research Institute, Menlo Park, California 94025*

Received March 18, 1971

The oxidation of propylene was investigated on silica-supported bismuth molybdate catalysts ( $\text{MoO}_3$ ,  $\text{Bi}_2\text{O}_3 \cdot 3\text{MoO}_3 + 0.25\text{Bi}_2\text{O}_3$ ,  $3\text{Bi}_2\text{O}_3 \cdot \text{MoO}_3$ , and  $\text{Bi}_2\text{O}_3$ ) by simultaneous measurement of the ESR spectra of the catalysts during the oxidation reaction at 325 and 390°C and the product distribution. As the oxygen/propylene ratio was increased in the range of 0.25 to 3, the  $\text{Mo}^{5+}$  signal intensity decreased and the total conversion increased. However, the acrolein selectivity remained almost constant. The  $\text{Mo}^{5+}$  signal intensity was found to be inversely proportional to the total propylene conversion. The experimental data are developed by assuming that the molybdenum ions detectable by ESR are primarily at the surface. These molybdenum ions in the  $\text{Mo}^{6+}$  valence state may be the surface sites necessary for the initial catalytic conversion step. Another type of site is postulated to account for selective oxidation to acrolein.

ESR was also employed to investigate the rates of oxidation and reduction of the catalysts by measurements of the  $\text{Mo}^{5+}$  signal and of the relative electrical conductivity of the samples. Very fast oxidation and reduction reactions with time constants of seconds are associated with oxidation and reduction involving the surface. Slow reduction reactions with time constants of half an hour are associated with reduction of the bulk with bulk diffusion as the probable rate-limiting process.

### INTRODUCTION

Electron spin resonance spectroscopy (ESR) of metal oxide catalysts during catalysis may be expected to provide information on the dependence of catalyst reactivity or selectivity on the metal cation valence state. To date, ESR measurements have been made on catalysts that were quenched to room temperature or lower after completion of kinetic measurements at elevated temperatures.

The literature contains several ESR studies of molybdenum oxide catalysts. Boreskov *et al.* (1) found a correlation between the yield of ethylene polymerization

and the intensity of the  $\text{Mo}^{5+}$  signal. They also postulated that an interaction with the alumina support stabilized the  $\text{Mo}^{5+}$  state with respect to reduction to  $\text{Mo}^{4+}$ . Seshadri and Petrakis (2) found that the catalytic activity for an aldol condensation and the intensity of the  $\text{Mo}^{5+}$  signal both showed the same functional dependence on the  $\text{MoO}_3$  content of catalysts which were pre-reduced in hydrogen. Cornaz *et al.* (3) examined the ESR spectra of oxygen-deficient  $\text{MoO}_3$  and of bismuth molybdate catalysts. The  $\text{Mo}^{5+}$  signal was found only in  $\text{MoO}_3$  at 77°K but not at room temperature, and the *g* value was reported to be 1.943. Peacock *et al.* (4) studied the ESR spectra of bismuth molybdate and  $\text{MoO}_3$  catalysts after exposure to propylene at reaction temperatures up to 500°C. However, the ESR spectra were taken after the catalyst had been quenched to room tem-

\* This study was sponsored by a group of industrial companies whose support is gratefully acknowledged.

† Permanent address: Asahi Chemical Industry Co., Ltd., Kawasaki, Japan.

perature, evacuated, and sealed off. A broad signal was observed with  $g_{\parallel} = 1.865$  and  $g_{\perp} = 1.933$ , which was ascribed to  $\text{Mo}^{5+}$ , and a narrow signal with  $g = 2.0036$ , which was considered to arise from carbon. In general, the  $\text{Mo}^{5+}$  signal intensity initially increased upon exposure of the catalyst to propylene. In some cases, depending on temperature and propylene pressure, the signal again decreased. When the bismuth molybdate catalyst was exposed at reaction temperatures to a 1:1 mixture of propylene and oxygen, the  $\text{Mo}^{5+}$  signal appeared after excess oxygen had been consumed. Masson and Nechtschein (5) used ESR to investigate the conditions for formation of  $\text{Mo}^{5+}$  in  $\text{MoO}_3/\text{Al}_2\text{O}_3$  catalysts that were exposed to hydrogen at elevated temperatures. The ESR spectra measured at room temperature displayed an unsymmetrical line at  $g = 1.95$ , which was attributed to  $\text{Mo}^{5+}$ . The  $\text{Mo}^{5+}$  signal intensity passed through a maximum as the amount of  $\text{MoO}_3$  supported on  $\text{Al}_2\text{O}_3$  was increased. The initial increase was attributed to formation of  $\text{Mo}^{5+}$  stabilized by interaction with  $\text{Al}_2\text{O}_3$ , and the subsequent decrease was attributed to a reaction in the concentrated  $\text{MoO}_3$  phase leading to formation of the nonparamagnetic  $\text{Mo}^{4+}$  ions. Seshadri *et al.* (6) investigated the combined effects of sulfiding with  $\text{H}_2\text{S}$  and of reducing with  $\text{H}_2$  molybdena on an alumina support and concluded that the sulfiding favors formation of  $\text{Mo}^{4+}$  at the expense of  $\text{Mo}^{5+}$ .

In the present study, ESR was employed to examine the catalyst at reaction temperatures with simultaneous analysis of the product gas. The system investigated was the oxidation of propylene in the presence of bismuth molybdate catalysts supported on silica gel. ESR was used (1) to monitor the intensity of the  $\text{Mo}^{5+}$  signal, and (2) to indicate relative changes of electrical conductivity of the catalyst. Gas mixtures containing various ratios of propylene and oxygen were passed over the catalyst, and the conversion and specificity were examined simultaneously with the ESR examination. Strong reducing atmospheres were avoided during catalysis partly because high conversion of propylene is observed at high  $\text{O}_2/\text{C}_3\text{H}_6$

ratios ( $\gamma$ ), and other evidence indicates that irreversible changes of the catalyst properties occur in strong reducing atmospheres.

#### EXPERIMENTAL DETAILS

The silica-supported catalysts have the following designations and compositions: M,  $\text{MoO}_3/77$  wt %  $\text{SiO}_2$ ; B/M-0.7,  $[\text{Bi}_2\text{O}_3 \cdot 3\text{MoO}_3 + 0.25\text{Bi}_2\text{O}_3]/50$  wt %  $\text{SiO}_2$ ; B/M-6,  $3\text{Bi}_2\text{O}_3 \cdot \text{MoO}_3/50$  wt %  $\text{SiO}_2$ ; and B,  $\text{Bi}_2\text{O}_3/55$  wt %  $\text{SiO}_2$ ; the number following the letter designation signifies the approximate bismuth/molybdenum atom ratio.

Catalyst B/M-0.7 was prepared by adding a solution of 2.12 g ammonium molybdate, 2.4 ml water, and 0.94 g of ammonium hydroxide ( $d = 0.88$  g/cm<sup>3</sup>) to 12.8 g of a silica sol (duPont's Ludox AS, 30 wt %). To this mixture a solution of 4.37 g bismuth nitrate dissolved in 5.3 ml of 5 N  $\text{HNO}_3$  was added. Catalyst B/M-6 was prepared by adding a mixture of 0.59 g ammonium molybdate, 0.66 ml water, and 0.26 g ammonium hydroxide solution to 17.2 g of silica sol. Then a solution of 9.70 g of bismuth nitrate in 11.7 ml 5 N  $\text{HNO}_3$  was added. Catalyst B was prepared by adding 9.2 g bismuth nitrate in 11 ml 5 N  $\text{HNO}_3$  to 18.2 g of silica sol. Catalyst M was prepared by adding a solution of 1.77 g ammonium molybdate, 2.0 ml water, and 0.79 g ammonium hydroxide to 1.59 g silica sol. The water from the above four catalyst suspensions was evaporated with stirring at low heat. The remaining solids were dried at 140°C overnight, and calcined in air at 540°C for 3 hr. The products were pressed into pellets, crushed, and sieved to obtain the size fraction between 32 and 40 mesh. All chemicals were reagent grade.

The quartz reactor shown in Fig. 1 consisted of an outer tube (3 mm i.d., 0.5 mm wall) with an inlet side arm for the reactant gases and a central outlet tube equipped with an unlubricated ground joint (lower tube dimensions 1 mm o.d., 0.2 mm wall) through which the reacted gases exited to the gas chromatograph. Quartz wool provided a means of maintaining the end of the central tube free of catalyst particles. About 0.1 g of catalyst filled the reactor to a height of about 2 cm.

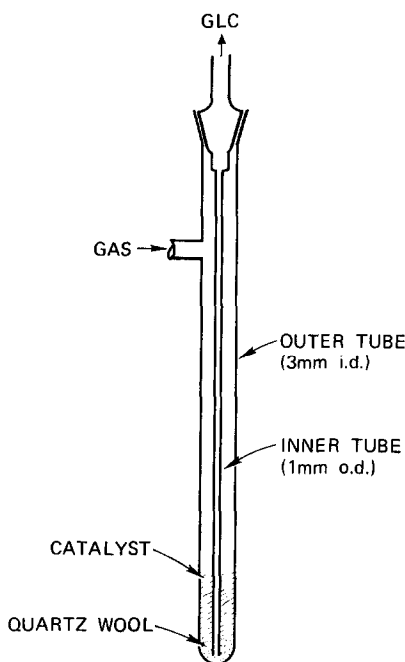


FIG. 1. Quartz reactor cell.

The reactor resided in a temperature-controlled quartz Dewar vessel (Varian V-4540) situated in the ESR cavity. Catalyst temperatures up to  $450^{\circ}\text{C}$  could be obtained by use of a heater coil twice the length of the standard one. A Variac controlled the power for heating the nitrogen flowing over the heater to the reactor. A thermocouple located within 2 cm of the cavity center monitored the reactor temperature. A fan was used to prevent excessive heating of the ESR cavity.

The total flow rate of propylene, oxygen, and helium was  $200\text{ cm}^3/\text{min}$ , but only 10 to  $20\text{ cm}^3/\text{min}$  of the gas mixture was bypassed through the reactor and its flow was monitored by a bubble flow meter. The gases from the reactor were analyzed by a gas chromatograph with two columns: Ucon at  $90^{\circ}\text{C}$  for separating acrolein and acetaldehyde, and silica gel at  $240^{\circ}\text{C}$  for separating oxygen, carbon dioxide, and propylene. The conversion is defined as the volume ratio of a given product to the propylene in the feed stream; selectivity is defined as the volume ratio of a given product to the propylene reacted.

ESR measurements were made with a Varian V-4502 X-band spectrometer equipped with a 12-in. magnet, a Fieldial, and a dual cavity ( $\text{TE}_{104}$ ) operated from the microwave bridge at about 200 mW. The reactor was inserted in one cavity modulated at  $10^5\text{ Hz}$  and 15 Oe. A sample of 0.1% pitch in KCl (Varian) was inserted in the other cavity modulated at 400 Hz to monitor the relative cavity sensitivity and to measure the  $g$  value. ESR spectra were measured at the reaction temperatures of 325 and  $390^{\circ}\text{C}$ . The absolute spin density of the  $\text{Mo}^{5+}$  resonance was evaluated by a first-moment analysis of the first derivative of the resonance line using a 0.1% pitch sample as an absolute spin standard. Unless otherwise specified, the signal intensity is expressed in terms of the relative peak-peak height of the resonance line at a given detector level and normalized for cavity sensitivity which depended upon the electrical conductivity of the sample, e.g., the degree of reduction.

## RESULTS

### ESR Signals

Two principal ESR signals were observed, and the first-derivative presentations are shown in Fig. 2 along with  $g$ -value markers. One signal was a broad asymmetric resonance, with  $g$  values in the range of 1.88 to 1.95, similar to that reported (1-5) for  $\text{Mo}^{5+}$ , and the other signal was a narrow resonance with a  $g$  value at 2.003 ascribed to carbon or a hydrocarbon radical (4). The composition of the reactant gas mixture influenced the shape of the broad line at high magnetic fields ( $g$  values 1.88 to 1.92) but not at low fields ( $g$  value 1.95). For catalyst B/M-0.7 at  $325^{\circ}\text{C}$ , curve (A) was obtained after the catalyst was exposed to propylene for 10 min. A narrower line (B) was observed a few minutes after oxygen was substituted for the propylene, but this effect is transient because oxygen soon causes the  $\text{Mo}^{5+}$  resonance to disappear completely. Under steady-state reaction conditions ( $\text{O}_2/\text{C}_3\text{H}_6$  ratios from 0.25 to 3), an intermediate line shape (C) was obtained, and peak-peak intensities of this

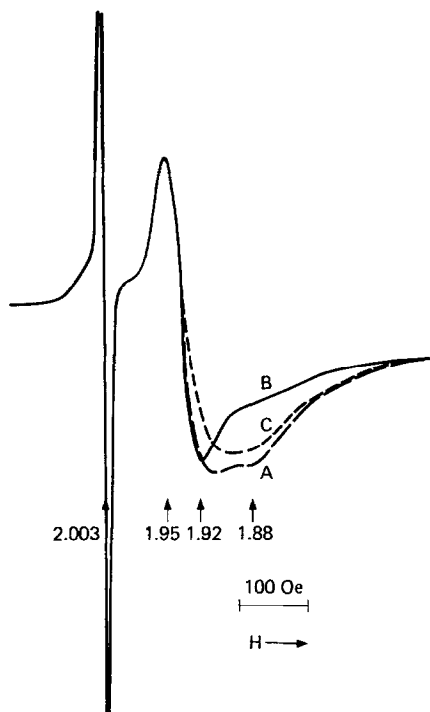


FIG. 2. ESR spectra of catalyst B/M-0.7 at 325°C. Curve A, after propylene reduction for 10 min; curve B, after subsequent exposure to oxygen for several minutes, and curve C, after exposure to an  $O_2/C_3H_6$  ratio of unity.

line ( $g$  values 1.95 and 1.90) were used as a measure of  $Mo^{5+}$  concentration.

The narrow ESR signal with a  $g$  value at 2.003 occurred only for catalysts containing bismuth and during exposure to gas mixtures of low  $O_2/C_3H_6$  ratios. For gas mixtures at a given  $O_2/C_3H_6$  ratio in contact with the catalyst, the signal intensity qualitatively increased with the bismuth content of the catalyst: the intensity was negligible for catalyst M, relatively small for B/M-0.7, and much stronger for catalysts B/M-6 and B. This observation provides some evidence that, in the presence of bismuth oxide, cracking of the hydrocarbon occurs. No hyperfine structure of this line could be detected, even when the catalyst during reaction was quenched to liquid nitrogen temperature.

#### $Mo^{5+}$ Signal and $O_2/C_3H_6$ Ratio

The steady-state value of the intensity of the signal for the catalysts M and B/M-

0.7 at 325°C changed reversibly and rapidly (within 1 min) when the ratio of  $O_2/C_3H_6$  in the feed stream was changed. But the signal intensity was essentially independent of the absolute amounts of these gases. The effect of the gas composition is shown in Fig. 3. These results were obtained by varying the propylene concentration at fixed oxygen-concentration levels of 3, 6, and 9 vol %. Although the mass of molybdenum in the two catalysts is equal, the  $Mo^{5+}$  signal intensity for catalyst M is about 50% higher than that for catalyst B/M-0.7 (Fig. 3).

The effect of catalyst temperature on the  $Mo^{5+}$  signal intensity was determined for an  $O_2/C_3H_6$  ratio of unity. As the temperature was increased from 325 to 390°C, the  $Mo^{5+}$  signal intensity for catalyst M changed from 80 to 165, and for catalyst B/M-0.7 from 47 to 15; for catalyst B/M-6 the signal intensity was determined only at 390°C and was 5.

The absolute spin density of the  $Mo^{5+}$  resonance was determined for catalyst B/M-0.7 (reaction temperature 325°C and gas composition 6 vol %  $C_3H_6$ , 6 vol %  $O_2$ , 88 vol % He) and found to be  $1.0 \times 10^{16}$  spins/g-catalyst; this spin density corresponds to 50 scale units of  $Mo^{5+}$  signal intensity. A Curie law correction was ap-

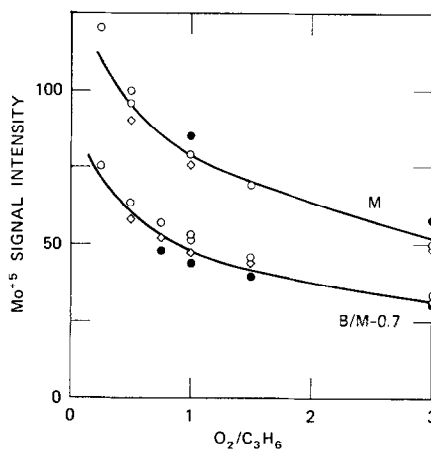


FIG. 3. Dependence of  $Mo^{5+}$  signal intensity on  $O_2/C_3H_6$  ratio at three constant oxygen concentrations for catalysts M and B/M-0.7 at 325°C ( $\circ$  = 3 vol %,  $\diamond$  = 6 vol %, and  $\bullet$  = 9 vol %  $O_2$ ).

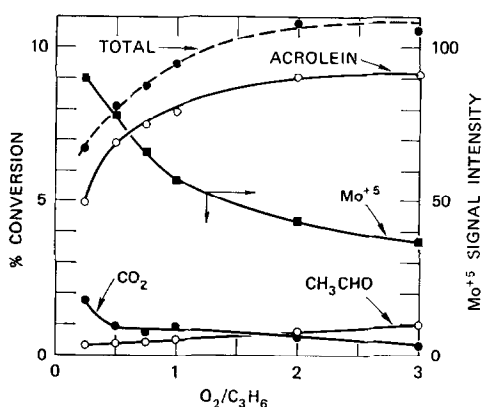


FIG. 4. Dependence of catalytic conversion and the  $\text{Mo}^{5+}$  signal intensity on  $\text{O}_2/\text{C}_3\text{H}_6$  ratio at 3 vol % propylene for catalyst B/M-0.7 at 325°C.

plied to compensate for the temperature difference between the catalyst and the spin standard (20°C). This spin density accounts for about  $4 \times 10^{-5}$  of the total mass of molybdenum of the catalyst. Assuming an area of  $1 \text{ m}^2/\text{g}$  for the bismuth-molybdate part of the catalyst, about 1% of the surface molybdenum sites were observed by ESR.

#### Conversion and Selectivity

The effects of the  $\text{O}_2/\text{C}_3\text{H}_6$  ratio on catalytic conversion and selectivity are shown in Figs. 4 and 5 for catalyst B/M-0.7 at 325°C, and the  $\text{Mo}^{5+}$  signal intensities measured during catalysis are also indicated. At 325°C oxidation of propylene could not be detected over catalyst M even though

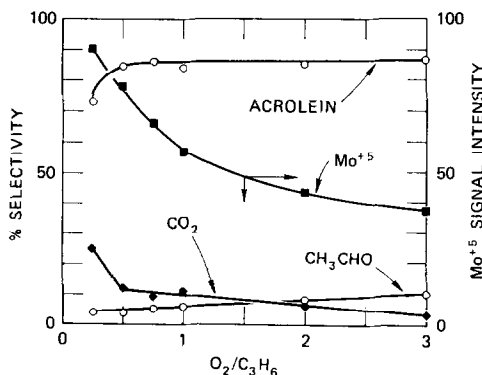


FIG. 5. Dependence of catalytic selectivity on  $\text{O}_2/\text{C}_3\text{H}_6$  ratio for catalyst B/M-0.7 at 325°C (same run as Fig. 4).

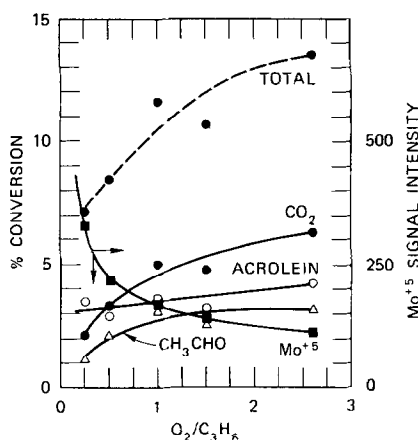


FIG. 6. Dependence of catalytic conversion and  $\text{Mo}^{5+}$  signal intensity on  $\text{O}_2/\text{C}_3\text{H}_6$  ratio at 3 vol % propylene for catalyst M at 390°C.

marked reversible changes in the intensity of the  $\text{Mo}^{5+}$  signal were observed as the  $\text{O}_2/\text{C}_3\text{H}_6$  ratio was altered (Fig. 3); however, oxidation was measurable at 390°C (Figs. 6 and 7) at which temperature the total conversion was about equal to that of catalyst B/M-0.7 at 325°C. In these runs the appropriate  $\text{O}_2/\text{C}_3\text{H}_6$  ratio was obtained by adjusting the propylene concentration while holding the oxygen concentration at 3 vol %. The values of percent conversion were obtained from analysis of the reactant gas. The conversion results for catalyst B/M-0.7 at 325°C (Fig. 4) and for catalyst M at 390°C

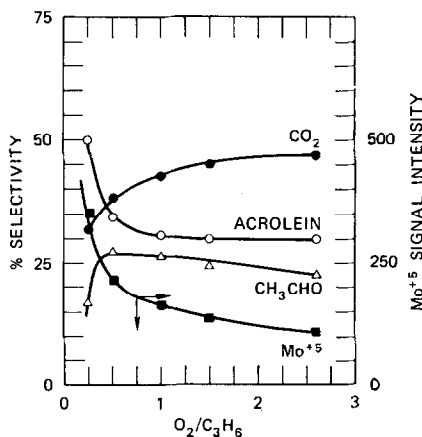


FIG. 7. Dependence of catalytic selectivity and the  $\text{Mo}^{5+}$  signal intensity on  $\text{O}_2/\text{C}_3\text{H}_6$  ratio for catalyst M at 390°C (same run as Fig. 6).

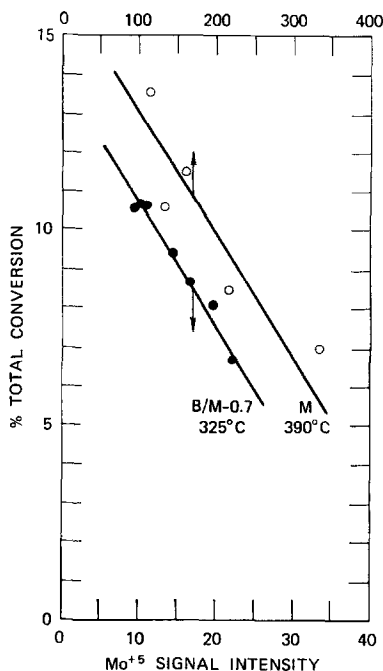


FIG. 8. Relationship between total conversion and  $\text{Mo}^{5+}$  signal intensity for catalyst M at  $390^\circ\text{C}$  and catalyst B/M-0.7 at  $325^\circ\text{C}$ .

(Fig. 6) suggest that a reciprocal relationship exists between total propylene conversion and the  $\text{Mo}^{5+}$  signal intensity, as demonstrated in Fig. 8. It should be noted that the  $\text{Mo}^{5+}$  signal intensities for catalysts B/M-0.7 and M differ by a factor of 1.5 at  $325^\circ\text{C}$  (Fig. 3) and by a factor of 10 at  $390^\circ\text{C}$  (Fig. 8). In the latter case the difference is undoubtedly due to the higher temperature rather than to a difference in surface area.

The selectivity for oxidation to acrolein, as well as to acetaldehyde and carbon dioxide, is essentially independent of the  $\text{O}_2/\text{C}_3\text{H}_6$  ratio and of the  $\text{Mo}^{5+}$  signal intensity for both catalysts M and B/M-0.7 (Figs. 5 and 7), except at the lowest  $\text{O}_2/\text{C}_3\text{H}_6$  ratio.

#### Evaluation of Rates of Reduction and Oxidation of the Catalysts

The rates of reduction and oxidation of bismuth molybdate catalysts have been determined separately by ESR and by electrical conductivity measurements (8-9).

It was of interest to use the ESR technique for both of these measurements on the catalyst employed during propylene oxidation. The rate of reduction of the catalyst can be determined by ESR by monitoring not only the  $\text{Mo}^{5+}$  signal intensity but also the relative changes in the electrical conductivity of the catalyst (10). Changes in electrical conductivity  $\Delta\sigma$  alter (1) the cavity sensitivity, which can be monitored by the changes in the intensity of a reference sample (in the present work the intensity  $I_p$  of 0.1% pitch in KCl was used) in the dual cavity, and (2) the microwave bridge balance, which can be monitored by the changes in the dc bias current of the crystal diode  $I_{cc}$ . It has been shown that  $\Delta\sigma$  is approximately proportional to  $\Delta(1/I_p)$  and to  $\Delta I_{cc}$  (10).

The results of such measurements show that when the catalysts at an elevated temperature are exposed to propylene, the initial very rapid increase of the  $\text{Mo}^{5+}$  signal intensity is followed by a much slower increase. The slow portion of the reduction process in propylene at  $390^\circ\text{C}$  is shown in Fig. 9 for the three catalysts initially pretreated in oxygen at this temperature. The results indicate that the bismuth molybdate catalysts are apparently more resistant to reduction than catalyst M. The ordinant of the curve for catalyst B/M-6 has been multiplied by a factor of 4.8 in order to

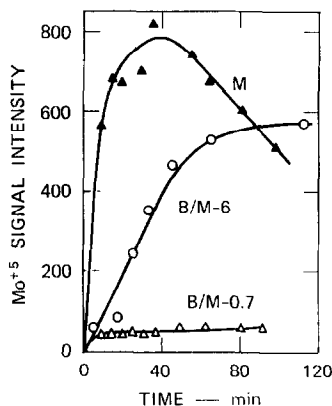


FIG. 9. Effect of propylene reduction on the  $\text{Mo}^{5+}$  signal intensity for three catalysts at  $390^\circ\text{C}$ . The ordinate for catalyst B/M-6 has been multiplied by a factor of 4.8.

normalize the data to the same molybdenum concentration as that of the other two catalysts. On this basis, catalyst B/M-0.7 is clearly the most resistant to reduction. The maximum of the  $\text{Mo}^{5+}$  signal for catalyst M upon extensive reduction is consistent with the interpretation that  $\text{Mo}^{5+}$  may be reduced to  $\text{Mo}^{4+}$  (4, 5). However, there are other reasons, which we will discuss presently, why ESR may not detect all  $\text{Mo}^{5+}$  ions.

Using  $I_p$  to monitor the changes in cavity sensitivity, the results in Fig. 10 show that  $I_p$  decreased during the reduction, i.e., the electrical conductivity of the samples increased. Reduction of bismuth oxide is also demonstrated by the results in Fig. 10; the reduction rate is initially slower than that of the other catalysts, but then accelerates. The relatively faster and larger change for catalyst M is consistent with the faster and larger extent of reduction shown by the data on the  $\text{Mo}^{5+}$  signal in Fig. 9. Thus, stability of the mixed oxides is again indicated. The increased electrical conductivity presumably results from formation of reduced species, such as  $\text{Mo}^{5+}$ ,  $\text{Mo}^{4+}$ , or  $\text{Bi}^{2+}$ , which act as electron donors to the conduction band. Upon subsequently exposing these catalysts at an elevated temperature to oxygen, the  $I_p$  value returned rapidly to its original high value.

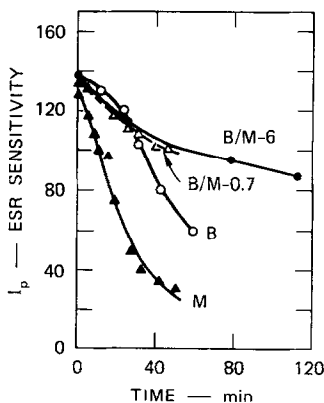
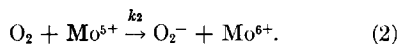
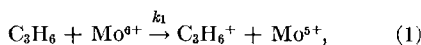


FIG. 10. Effect of propylene reduction of four catalysts at 390°C on ESR sensitivity as indicated by  $I_p$ , the signal intensity of a pitch sample in the reference cavity. Same run as Fig. 9, except catalyst B.

Finally, an attempt to determine the rates of reducibility and oxidizability was made by recording changes in the crystal current  $I_{cc}$ . Easily measurable and reversible changes of this quantity occurred when the  $\text{O}_2/\text{C}_3\text{H}_6$  ratio was suddenly changed between high and low values. However, under our experimental conditions it was not possible to alter the gas composition fast enough to provide a "step-function" concentration gradient. For example, for catalyst B/M-0.7 at 390°C, when the  $\text{O}_2/\text{C}_3\text{H}_6$  ratio was changed between  $\infty$  and 1, the half-time for a change in  $I_{cc}$  decreased with an increase in gas flow rate; for the largest practical flow rate of 60  $\text{cm}^3/\text{min}$  (contact time of 0.15 sec) the half-time was 6 sec. The rate of change of  $I_{cc}$  was probably still limited by a gas diffusion process, and, therefore, the actual rates of oxidation and reduction could not be measured. For catalysts B and B/M-0.7, the magnitude and rate of change of  $I_{cc}$  was qualitatively similar when the  $\text{O}_2/\text{C}_3\text{H}_6$  was varied between  $\infty$  and 1.

#### DISCUSSION

For each of the catalysts (B/M-0.7 and M) investigated, the experimental results demonstrate that under steady-state conditions the extent of propylene conversion and the intensity of the  $\text{Mo}^{5+}$  signal are affected by the  $\text{O}_2/\text{C}_3\text{H}_6$  ratio. Most likely this ratio of reactants governs the distribution of surface molybdenum ions, such as  $\text{Mo}^{5+}$  and  $\text{Mo}^{6+}$ , in different valence states, as a result of a sequence of reactions involving charge transfer such as:



Based on these reactions the steady-state condition leads to the following relationship between the valence states of molybdenum and the reactant concentrations

$$\frac{[\text{Mo}^{6+}]}{[\text{Mo}^{5+}]} = \frac{k_2 [\text{O}_2]}{k_1 [\text{C}_3\text{H}_6]}$$

which is in agreement with experimental observations. A measure of the relative distribution of  $\text{Mo}^{6+}$  and  $\text{Mo}^{5+}$  can be derived from the fact that the total number

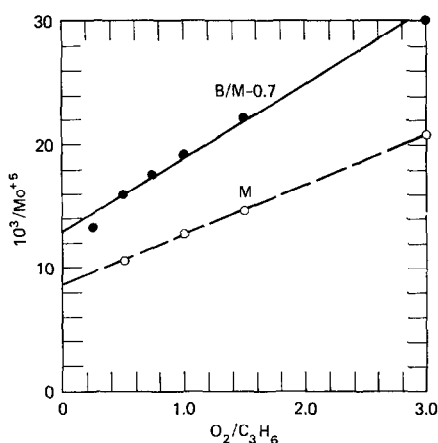


FIG. 11. The dependence of  $1/Mo^{5+}$  on  $O_2/C_3H_6$  ratio for catalysts M and B/M-0.7 at  $325^\circ C$  (data taken from Fig. 3).

of molybdenum surface sites  $N_s$  is fixed for a given catalyst sample,

$$Mo^{5+} + Mo^{6+} = N_s \quad (3)$$

Since at vanishing ratios of  $O_2/C_3H_6$ ,  $Mo^{5+}$  would be expected to predominate on the surface, a graphical analysis of the data presented in Fig. 3 allows evaluation of the maximum surface density of  $Mo^{5+}$  by plotting the reciprocal of the  $Mo^{5+}$  signal intensity vs the  $O_2/C_3H_6$  ratio (Fig. 11). The intercept with the ordinate yields the value of  $N_s$  since under these conditions all molybdenum is present as  $Mo^{5+}$ . Once  $N_s$  has been evaluated in this manner, we can compute the relative magnitude of  $[Mo^{6+}]$  from the difference between  $N_s$  and the observed  $Mo^{5+}$  signal intensity at different  $O_2/C_3H_6$  ratios. Such an analysis of the data is presented in Fig. 12 for the two catalysts under examination. Based on this analysis the ratio  $[Mo^{6+}]/[Mo^{5+}]$  appears to be a linear function of the  $O_2/C_3H_6$  ratio for both catalysts B/M-0.7 and M. This observation lends further support to the assumption that the molybdenum ions detected by ESR (although a small fraction of the total molybdenum) are either in  $Mo^{6+}$  or  $Mo^{5+}$  state and probably at the surface of the catalysts. In addition, the ratio of the two rate constants  $k_2/k_1$  is the same for both catalysts at the same temperature. Since for catalyst M no measurable conversion of

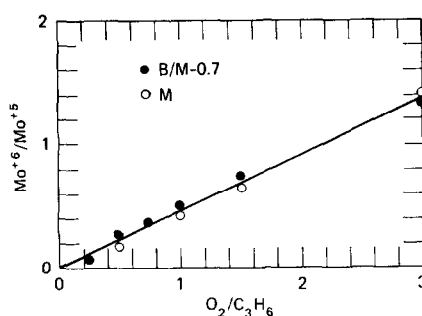


FIG. 12. The relationship between  $Mo^{6+}/Mo^{5+}$  and the  $O_2/C_3H_6$  ratio for catalysts M and B/M-0.7 at  $325^\circ C$  (data taken from Fig. 11).

propylene was detectable at  $325^\circ C$ , although the  $Mo^{6+}/Mo^{5+}$  exhibited variations with the  $O_2/C_3H_6$  ratio, it must be concluded that the charge transfer steps [Eqs. (1) and (2)] are not rate determining in the process of propylene oxidation. At the same time the results indicate that  $Mo^{6+}$  sites, and/or the oxygen species associated with the  $Mo^{6+}$  site, are essential for propylene oxidation and that the conversion rate is high when the relative  $Mo^{6+}$  surface density is high, i.e., low  $Mo^{5+}$ . Examination of the product distribution points to the interesting fact that selectivity of each of the catalysts for acrolein formation does not appear to be tied in with the  $Mo^{6+}/Mo^{5+}$  distribution detectable by ESR. Although catalyst B/M-0.7 exhibits much higher acrolein selectivity at  $325^\circ C$  than catalyst M at  $390^\circ C$ , the selectivity of each catalyst remains relatively constant and unaffected by the  $O_2/C_3H_6$  ratio. The initial attack of the  $C_3H_6$  molecule appears to involve a  $Mo^{6+}$  type site, deduced from the ESR data, which is common to both catalysts, but the subsequent oxidation steps leading to specific products are governed by other variables. For example, in the mixed oxide catalyst, the role of  $Bi^{3+}$  has been explored in several recent studies (11-13) in terms of a dual-site mechanism. We consider it significant that catalyst B/M-0.7, which yields high acrolein selectivity, also exhibits high stability for reduction of  $Mo^{6+} \rightarrow Mo^{5+}$  on exposure to propylene (Figs. 9 and 10). An opposite effect was reported for reduction of such catalysts by hydrogen (13). Cation valence



stabilization by admixture of foreign metal oxides (14) and by catalyst moderators (15) emerges as an important factor in selective oxidation catalysis. As suggested in Refs. (15) and (16), such valence stabilization affects the electronic properties of the catalyst and thereby influences the charge distribution of reactant species on the surface of the catalyst. Thus the degree of propylene oxidation or the selectivity of the catalyst may be reflected in the type of oxygen species (e.g., O, O<sup>-</sup>, or O<sub>2</sub><sup>-</sup>) preponderant on the catalyst surface.

The paramagnetic species giving rise to the Mo<sup>5+</sup> signal may, of course, be either at the surface or in the bulk. However, during catalysis the evidence favors their location at the surface. This conclusion is based on the qualitative observation that when the O<sub>2</sub>/C<sub>3</sub>H<sub>6</sub> ratio is changed, very rapid changes occur in both the initial change of the Mo<sup>5+</sup> signal intensity and the microwave bridge crystal diode current. By contrast, reduction of molybdenum in the bulk may occur slowly under reducing conditions. For example, such bulk reduction may account in part for the relatively large values of the Mo<sup>5+</sup> signal intensity resulting from exposure of catalyst M to propylene (Fig. 9) in comparison to those found with the presence of some oxygen (Fig. 3). Reduction of the bulk is undoubtedly also indicated by the slow changes of the Mo<sup>5+</sup> signal (especially for catalyst M), and of the cavity sensitivity parameter  $I_p$  (Figs. 9 and 10). Similar slow changes have been reported for the Mo<sup>5+</sup> signal (4, 5) and electrical conductivity (7, 8). Incidentally, severe reduction of bismuth molybdate during propylene oxidation has been reported by Keulks (17). But his results with a pre-reduced sample of bismuth molybdate exposed to a gas mixture containing a ratio of O<sub>2</sub>/C<sub>3</sub>H<sub>6</sub> < 0.76 are more indicative of the competitive oxidation rate of catalyst vs olefin. In any case, the slow oxidation and reduction reactions in question are probably rate limited by a bulk diffusion process which, in turn, is determined by crystal structure and composition. Bismuth oxide itself is oxidized or reduced in a way qualitatively comparable to the

bismuth molybdates. For example, for catalyst B surface oxidation or reduction is indicated by the rapid change of the crystal diode current resulting from changes in the O<sub>2</sub>/C<sub>3</sub>H<sub>6</sub> ratio; bulk reduction by propylene is indicated by the slow change of the  $I_p$  parameter (Fig. 10). These results are in qualitative agreement with those obtained from electrical conductivity (8). From past experience with ZnO (10), the changes of  $I_p$  resulting from reduction of catalyst M for 1 hr (Fig. 10) correspond to an increase of ionized donors by an order of magnitude of 10<sup>16</sup> to 10<sup>17</sup> cm<sup>-3</sup>, and this donor density is equivalent to the reduction of about 10<sup>-8</sup> to 10<sup>-7</sup> moles of bismuth or molybdenum per gram of catalyst. Hence the amount of reduction, which is probably mostly in the bulk, is very small but is readily detected by this sensitive technique.

It is of interest to inquire whether all the surface Mo<sup>5+</sup> ions are detectable by ESR. This question arises partly because of the apparently low absolute concentration of Mo<sup>5+</sup> ions observed and also because several mechanisms are known that may "attenuate" the signal. Three of these mechanisms are: (1) instability of Mo<sup>5+</sup> with respect to reduction to Mo<sup>4+</sup>, (2) magnetic dipolar relaxation processes, and (3) crystal field effects.

Regarding the first mechanism, it has been reported (4-6) that Mo<sup>5+</sup> ions are unstable with respect to reduction to Mo<sup>4+</sup>, especially for MoO<sub>3</sub> not in contact with a support such as activated alumina (1, 5, 6). Accordingly, the maximum of the Mo<sup>5+</sup> signal intensity observed during reduction of MoO<sub>3</sub> in propylene (Fig. 9) may result from initial reduction of Mo<sup>6+</sup> to Mo<sup>5+</sup> followed by further reduction to the non-paramagnetic Mo<sup>4+</sup>, an explanation which follows Peacock *et al.* (4). However, reduction to Mo<sup>4+</sup> is less likely to occur when the O<sub>2</sub>/C<sub>3</sub>H<sub>6</sub> ratio is not too low: (a) Mo<sup>5+</sup> signal intensities are reversible (Fig. 3); (b) the response of the crystal diode current to changes in gas composition is also reversible; and (c) the decrease of the Mo<sup>5+</sup> signal intensity upon reduction of catalyst M in pure propylene occurs only after an initial substantial rise, suggesting that adequate

bulk  $\text{Mo}^{5+}$  is required before further reduction occurs.

The second mechanism occurs when the  $\text{Mo}^{5+}$  concentration is sufficiently large that magnetic dipolar interactions cause substantial line broadening. This mechanism is probably not active, even during extensive reduction of catalyst M (Fig. 9) where the concentration of  $\text{Mo}^{5+}$  ions becomes greater than the other catalysts, because significant line broadening is not apparent. The broad line observed during catalysis (Curve C, Fig. 2), which is similar to that observed during reduction in propylene (Curve A), suggests the presence of two paramagnetic centers. For example, the component at a  $g$  value of 1.88 may be ascribed to easily oxidizable  $\text{Mo}^{5+}$  ions at the surface, and the component at 1.92, which is the last to disappear during oxidation, may be due to  $\text{Mo}^{5+}$  ions, perhaps below the surface, which oxidize more slowly. Two forms of  $\text{Mo}^{5+}$  have been postulated to account for the complex structure of this resonance line observed in MgO containing molybdenum (18), and catalyst pretreatment has been shown to affect line shape (2).

The influence of crystal field splitting is a third mechanism by which transition paramagnetic ions may not be detectable by ESR. It has been predicted that when  $\text{Mo}^{5+}$  ions are in a crystal field of octahedral symmetry, their detection by ESR requires very low temperatures; however, in fields of dodecahedral symmetry the  $4d$  orbital levels are split into a lower singlet and an upper quartet with a large energy difference so that ESR at elevated temperatures is possible (19). Maksimovskaya *et al.* (20) conclude that, for molybdate catalysts, ESR detection of  $\text{Mo}^{5+}$  ions at room temperature is possible because a crystalline field of low symmetry exists about the ions. We may, therefore, speculate that the favorable crystalline field splitting occurs in the case of some surface  $\text{Mo}^{5+}$  ions and makes detection possible for the surface ions, even at elevated temperatures. The determination of the magnitude of the splittings requires knowledge of the crystal field symmetry and the magnitude and distortion of the electric field about the  $\text{Mo}^{5+}$  surface ions; such

considerations are beyond the scope of this paper.

### CONCLUSIONS

The present study shows that useful information may be obtained by correlating the ESR properties of related catalysts during catalytic propylene oxidation with the catalytic conversion rates and selectivities. Based on the reciprocal relationship between total conversion and the  $\text{Mo}^{5+}$  signal intensity, it is proposed that  $\text{Mo}^{6+}$  type sites are required for conversion reactions, perhaps for the initial oxidative dehydrogenation step. Based on the absence of correlation between the selectivity and the  $\text{O}_2/\text{C}_3\text{H}_6$  ratio or the  $\text{Mo}^{5+}$  signal intensity, it is proposed that another surface site, which is not detectable by ESR, controls the selectivity. Several considerations favor assignment of the observable  $\text{Mo}^{5+}$  species to surface sites, especially during catalysis; however, some  $\text{Mo}^{5+}$  species may be detectable in the bulk especially when the catalyst is reduced in propylene alone.

A study of the reduction rates of the catalysts, by means of the  $\text{Mo}^{5+}$  signal and the electrical conductivity parameters, points toward the existence of an initial rapid reaction which is probably at the surface, and of a subsequent slow reaction which may involve bulk species or at least difficulty reducible surface species. These results also show that the bismuth molybdate catalyst, B/M-0.7, which exhibits the greatest acrolein conversion rate and selectivity, is also the most stable toward the slow reduction. It may be concluded that this composition among the bismuth molybdate catalysts studied provides optimal stabilization of the  $\text{Mo}^{6+}$  valence state.

### REFERENCES

1. BORESKOV, G. K., DZISKO, V. A., EMELYANOVA, V. M., PECHERSKAYA, Y. I., AND KAZANSKII, V. B., *Dokl. Akad. Nauk SSSR* **150**, 829 (1963).
2. SESHADRI, K. S., AND PETRAKIS, L., *J. Phys. Chem.* **74**, 4102 (1970).
3. ÇORNAZ, P. F., VAN HOFF, J. H. C., PLUIJM, F. J., AND SCHUIT, G. A. S., *Discuss. Faraday Soc.* **41**, 290 (1966).

4. PEACOCK, J. M., SHARP, M. J., PARKER, A. J., ASHMORE, P. G., AND HOCKEY, J. A., *J. Catal.* **15**, 379 (1969).
5. MASSON, J., AND NECHTSCHNEIN, J., *Bull. Soc. Chim. Fr.* **10**, 3933 (1968).
6. SESHADRI, K. S., MASSOTH, F. E., AND PETRAKIS, L., *J. Catal.* **19**, 95 (1970).
7. CALLAHAN, J. L., GRASELLI, R. K., MILBERGER, E. C., AND STRECKER, H. A., *Ind. Eng. Chem., Prod. Res. Develop.* **9**, 134 (1970).
8. PEACOCK, J. M., PARKER, A. J., ASHMORE, P. G., AND HOCKEY, J. A., *J. Catal.* **15**, 387 (1969).
9. PLUTA, J., *Z. Anorg. Allg. Chem.* **356**, 105 (1967).
10. SANCIER, K. M., *J. Catal.* **16**, 44 (1970).
11. BATIST, P. A., LIPPENS, B. C., AND SCHUIT, G. C. A., *J. Catal.* **5**, 55 (1966).
12. SAKAMOTO, T., EGASHIRA, M., AND SEIYAMA, T., *J. Catal.* **18**, 407 (1970).
13. SACTLER, W. M. H., AND DEBOER, N. H., *Proc. Int. Congr. Catal. 3rd, (1964)*, p. 254 (1965).
14. INAMI, S. H., AND WISE, H., *J. Catal.* **18**, 343 (1970).
15. WOOD, B. J., AND WISE, H., *J. Catal.* **15**, 355 (1969).
16. HOLBROOK, L., AND WISE, H., *J. Catal.* **20**, 367 (1971).
17. KEULKS, G. W., *J. Catal.* **19**, 232 (1970).
18. KRYLOV, O. V., AND MARGOLIS, L. Y., *Kinet. Catal.* **11**, 358 (1970).
19. AYSOUGH, P. B., "Electron Spin Resonance in Chemistry," p. 193. Methuen, London, 1967.
20. MAKSIMOVSKAYA, R. I., ANUFRIENKO, V. F., AND KOLOVENTNOV, G. D., *Kinet. Catal.* **9**, 984 (1968).